Spectral characterisation of colour printer based on a novel grey component replacement method

Jinyi Guo (郭晋一)[1,2], Haisong Xu (徐海松)[1*], M. Ronnier Luo[2], and Binyu Wang (王彬宇)[1,2]

[1]*State Key Laboratory of Modern Optical Instrumentation, Zhejiang University, Hangzhou 310027, China*

[2]*Department of Colour Science, University of Leeds, Leeds LS2 9JT, UK*

[*]*Corresponding author: chsxu@zju.edu.cn*

Received January 24, 2011; accepted March 3, 2011; posted online May 12, 2011

Conventional printer characterisation models are generally based on the assumption that the densities of primary colours are additive. However, additivity failure frequently occurs in practice. We propose a novel grey component replacement (GCR) method based on the spectral density sub-additivity equations in this letter for spectral characterisation of a 4-ink colour printer. The method effectively correct the error caused by additivity failure. Real high-quality hardcopy samples are produced as evidence of the feasibility of the proposed method and to evaluate the model performance. Finally, the GCR model for characterising colour printer with high spectral and colorimetric prediction accuracy is established.

OCIS codes: 330.1690, 330.1715, 330.1730, 300.6550.

doi: 10.3788/COL201109.073301.

In the typical cyan, magenta, yellow, and black (CMYK) 4-ink colour printer, the use of black ink offers many advantages, such as low cost, wider colour gamut, improved image sharpness[1], etc. As a subtractive colour system, the combination of cyan, magenta, and yellow colours is substituted by the black colour. Grey component replacement (GCR) and under colour removal (UCR) technologies are extensively used for black generation[2,3]. These could be applied further in the spectral characterisation model of colour printer for recovery of spectral reflectance of colour target and avoidance of metamerism[4,5].

Colour density represents the absorption of the colour surface. It has several expressions including spectral density and colorimetric density[6], and the former could be calculated as

$$D(\lambda) = \lg \frac{R_0(\lambda)}{R(\lambda)}, \tag{1}$$

where $D(\lambda)$ is the spectral density of the target colour at wavelength λ, $R_0(\lambda)$ and $R(\lambda)$ are the spectral reflectance of the substrate (white paper) and the target colour at wavelength λ, respectively.

Generally, the conventional GCR method is based on the assumption that the primary colour densities are additive[3,4]. However, the additivity does not exactly hold in practice and the so-called additivity failure frequently occurs[7]. These occurrences could be caused by plenty of reasons, such as the complex interaction between ink and paper, light scattering, halftone structure, etc. In the study of Zeng[4], colorimetric density was used to implement the GCR method for direct colorimetric mapping. To solve the problem caused by the additivity failure, the author proposed a refinement algorithm by simply adjusting cyan, magenta, and yellow (CMY) values to compensate for the density additivity error and to keep the K value unchanged according to a feedback process. For the purpose of spectral colour reproduction, specific to the spectral density in this letter, the phenomenon of additivity failure was explored and a novel set of sub-additivity equations was proposed to correct the problem. The equations were applied further in the GCR method to characterise the CMYK 4-ink printer for precise spectral mapping.

To investigate the additivity failure phenomenon and deduce the sub-additivity equations, 100 training samples were printed as shown in Fig. 1. The normalised ink amount values are listed in Table 1 by a typical CMYK 4-ink colour printer (HP Designjet 1055 CM, Japan). The 10 levels of ink amount values in Table 1 were designed to obtain samples uniformly distributed in the CIELAB L^* lightness according to the tone reproduction curves of the CMYK channels. The ink amount could be directly controlled by 'Adobe PostScript' page description language, which allows the production of samples with precise normalised ink amount values for modelling. The samples in the same column had the same CMY values and those in the same row had the same K values. Spectral reflectances of the entire 100 samples were measured by a GretagMacbeth Spectrolino spectrophotometer with the spectral range of 380–730 nm at 10-nm intervals. Subsequently, the spectral densities at each wavelength of all the samples were calculated by Eq. (1).

Note that the CMY values of the samples in the first column of Fig. 1 are 0. Therefore, a one-dimensional (1D) look up table (LUT) formulated from the black ink

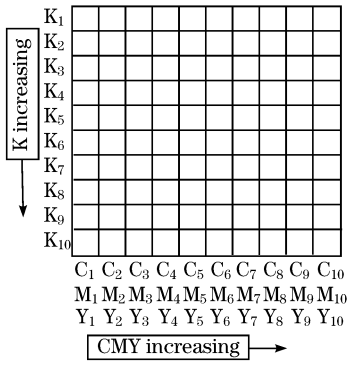

Fig. 1. Sketch of 100-training samples used in the investigation of additivity failure and deduction of sub-additivity equations.

Table 1. Normalised CMYK Values of 100 Training Samples

Level(n)	C$_n$	M$_n$	Y$_n$	K$_n$
1	0	0	0	0
2	0.0581	0.1018	0.0593	0.0811
3	0.1439	0.2045	0.1347	0.1402
4	0.2216	0.3023	0.208	0.2377
5	0.3111	0.3915	0.2986	0.3402
6	0.4189	0.5131	0.3784	0.4471
7	0.5557	0.6247	0.5067	0.5831
8	0.7028	0.7502	0.7164	0.7165
9	0.8604	0.8726	0.8536	0.8641
10	1	1	1	1

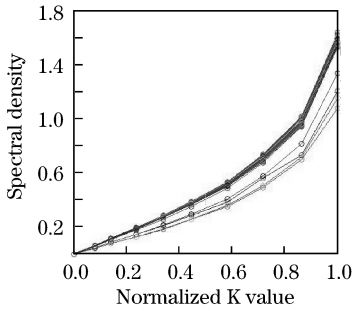

Fig. 2. 1D LUT from normalized K to spectral density.

normalised to spectral density values could be obtained by interpolation based on the spectral data of the samples in the first column. In Fig. 2, the 36 curves represent the relation between the normalised K value and the corresponding spectral density at each of the 36 wavelengths (from 380 to 730 nm at 10-nm intervals).

From column 2 to 10 of Fig. 1, each group of 10 samples in the same column has exactly the same CMY values and increasing K values from top to bottom. The spectral density of the 4-ink combination D_{CMYK} is plotted in Fig. 3 against the density of the added black ink D_{K} for the samples in each column. Due to the large number of spectral data, only the results at several typical wavelengths, i.e., 430, 540, and 700 nm (close to the CIE1931 blue, green, and red primary wavelengths, respectively), are plotted in Fig. 3. Data at other wavelengths showed similar trends.

Each curve containing 10 points at each wavelength of Fig. 3 is derived from the 10 samples of each column of the training samples. Assuming the spectral densities were additive in the ideal case, the additivity equation of $D_{\mathrm{CMYK}} = D_{\mathrm{CMY}} + D_{\mathrm{K}}$ should fully satisfy the requirement that all the curves were straight lines parallel to the ideal 45° line. However, results show that the additivity could roughly hold for the left end of the curves with small density values, but apparent additivity failure occurred when saturation of the density occurred toward the right end of the curves, especially when $D_{\mathrm{K}} > 1$. This indicates that the additivity failure appears mostly at the high colour density region because saturation of the ink coverage on the substrate is occurring.

To correct the errors caused by the additivity failure and predict the density of the mixing colour from each individual colour, a novel set of sub-additivity equations were proposed to predict the 4-ink density D_{CMYK} according to the 3-ink density D_{CMY} and the added black ink density D_{K}. The process is illustrated as follows. The 100-training samples in different columns had different initial 3-ink spectral densities D_{CMY} (when K=0). Densities were denoted as $D_{\mathrm{CMY}}(\lambda)_i$ (i=1, 2, $\cdots$, 10), where i represents the column number. For each curve, the relationship between D_{CMYK} and D_{K} was calculated by applying cubic spline interpolation as

$$D_{\mathrm{CMYK}}(\lambda)_i = f_i(D_{\mathrm{K}}(\lambda)_i) \quad . \tag{2}$$

For any 4-ink mixing colour with known D_{CMY} and D_{K}, the closest columns of training samples should be confirmed first according to the 3-ink density value of D_{CMY}. Subsequently, its 4-ink density D_{CMYK} could be calculated by the following sub-additivity equations

$$D_{\mathrm{CMYK}}(\lambda) = D_{\mathrm{CMYK}}(\lambda)_i + \frac{\{f_{i+1}[D_{\mathrm{K}}(\lambda)] - f_i[D_{\mathrm{K}}(\lambda)]\}[D_{\mathrm{CMY}}(\lambda) - D_{\mathrm{CMY}}(\lambda)_i]}{D_{\mathrm{CMY}}(\lambda)_{i+1} - D_{\mathrm{CMY}}(\lambda)_i}$$

when $D_{\mathrm{CMY}}(\lambda)_i < D_{\mathrm{CMY}}(\lambda) < D_{\mathrm{CMY}}(\lambda)_{i+1}$, $i = 1, 2, \cdots, 9$; (3)

$D_{\mathrm{CMYK}}(\lambda) = f_1[D_{\mathrm{K}}(\lambda)]$, when $D_{\mathrm{CMY}}(\lambda) < D_{\mathrm{CMY}}(\lambda)_1$; (4)

$D_{\mathrm{CMYK}}(\lambda) = f_{10}[D_{\mathrm{K}}(\lambda)]$, when $D_{\mathrm{CMY}}(\lambda) > D_{\mathrm{CMY}}(\lambda)_{10}$; (5)

$D_{\mathrm{CMYK}}(\lambda) = f_i[D_{\mathrm{K}}(\lambda)]$, when $D_{\mathrm{CMY}}(\lambda) = D_{\mathrm{CMY}}(\lambda)_i$, $i = 1, 2, \cdots, 10$. (6)

For the investigation of the performance of the proposed sub-additivity equations in predicting the spectral density of mixing colour, Table 2 lists the detailed prediction results of 10 testing samples. Due to the large number of spectral data, only the spectral densities at 540 nm are presented. Nevertheless, results for other wavelengths showed similar trends.

In Table 2, the significant additivity failure occurred

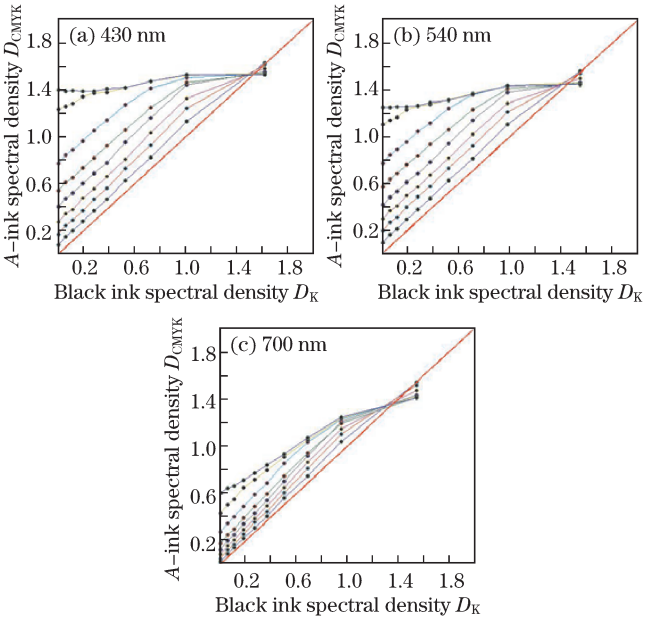

Fig. 3. Relationship between the 4-ink spectral density D_{CMYK} and the added black ink spectral density D_{K}. (a) 430, (b) 540, and (c) 700 nm.

for samples 7 and 10 because the 4-ink densities calculated by their additivity equations were 2.1386 and 1.9081, respectively, whereas their measured densities (1.4953 and 1.4740) were distinctly different. However, the predicted densities derived by sub-additivity equations of the two samples (1.4492 and 1.4843) were quite close to the measured values. This indicates that the proposed sub-additivity equations effectively corrected the error caused by the additivity failure. The predicted densities obtained by sub-additivity equations were always closer to the actual densities than those calculated by additivity equation. Moreover, satisfactory prediction performance was achieved.

Figure 4 shows the flowchart for characterising the CMYK printer when the sub-additivity equations to the GCR method to correct the additivity failure is applied. For the reproduction of a desired set of spectral reflectances $R(\lambda)$, the spectral density $D(\lambda)$ at each wavelength is calculated by Eq. (1) first. This is followed by deriving the potential black ink value $\mathrm{K_{max}}$ using $D(\lambda) \geqslant D_{\mathrm{Kmax}}(\lambda)$ at all wavelengths, where $D_{\mathrm{Kmax}}(\lambda)$ is the corresponding spectral density of $\mathrm{K_{max}}$ at wavelength λ. $\mathrm{K_{max}}$ represents the maximum black ink amount that can be used for reproducing the target colour. The derivation was performed according to the established 1D LUT for the black ink from its normalised value to spectral density. Subsequently, the black ink value K actually used for printing is calculated by

$$\mathrm{K} = p\mathrm{K_{max}}, \tag{7}$$

where p is the GCR percentage and could be determined by

$$p = w\mathrm{K}^{\gamma}_{\mathrm{max}}, \tag{8}$$

where w is the GCR weighting coefficient, $0 \leqslant w \leqslant 1$; γ is the correcting factor which defines the curve shape, $\gamma \geqslant 1$.

After the actual K value is confirmed, the black ink density $D_{\mathrm{K}}(\lambda)$ can be obtained by the black ink 1D LUT from its normalised value to spectral density. The 3-ink density $D_{\mathrm{CMY}}(\lambda)$ is then calculated from 4-ink density $D(\lambda)$ and black ink density $D_{\mathrm{K}}(\lambda)$ by inverting the sub-additivity equations described previously.

Inverting the sub-additivity equations to calculate the 3-ink density $D_{\mathrm{CMY}}(\lambda)$ requires the determination of the closest columns of training samples according to the 4-ink density $D(\lambda)$. Preliminarily, the corresponding 4-ink densities $f_i[D_{\mathrm{K}}(\lambda)], i = 1, 2, \cdots, 10$ in each of the 10 columns of the training samples in Fig. 1 are calculated from the known black ink density $D_{\mathrm{K}}(\lambda)$ by Eq. (2). Consequently, the 3-ink density $D_{\mathrm{CMY}}(\lambda)$ can be calculated according to the following inverse sub-additivity equations:

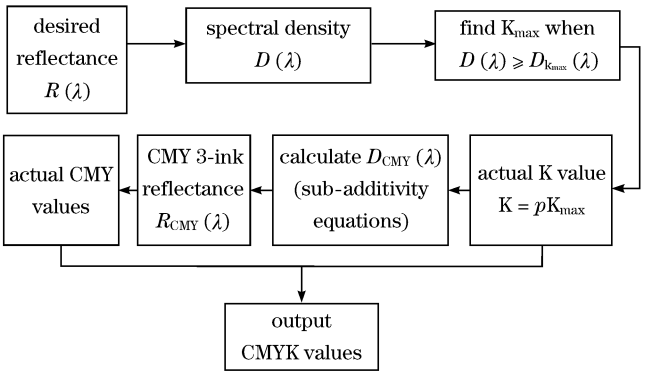

Fig. 4. Flowchart of the GCR method for the characterisation of CMYK colour printer.

Table 2. Prediction Results of Sub-additivity Equations for 10 Testing Samples (Spectral Densities at Wavelength of 540 nm)

Sample Number	1	2	3	4	5	6	7	8	9	10
C	0.3333	0	0.6667	0	0	0.6667	0.6667	0.3333	0	0.3333
M	0.3333	0.6667	0.6667	0	0.6667	0	1	0.6667	0.3333	0.3333
Y	0.3333	0.3333	0.3333	0.6667	0	0	0.3333	0.6667	0.3333	0.3333
K	0.3333	0.3333	0.3333	0.3333	0.6667	0.6667	0.6667	0.6667	0.6667	1
D_{CMY}	0.3575	0.6914	0.8783	0.0181	0.6543	0.1655	1.5075	0.8111	0.2846	0.3575
D_{K}	0.2681	0.2681	0.2681	0.2681	0.6311	0.6311	0.6311	0.6311	0.6311	1.5506
Additivity $D_{\mathrm{K}}+D_{\mathrm{CMY}}$	0.6256	0.9595	1.1464	0.2862	1.2854	0.7966	2.1386	1.4422	0.9157	1.9081
Measured D_{CMYK}	0.6305	0.9191	1.1100	0.3403	1.1759	0.8149	1.4953	1.3242	0.9280	1.4740
Predicted D_{CMYK}	0.6259	0.9537	1.1082	0.2887	1.2260	0.8161	1.4492	1.3168	0.9300	1.4843
Relative Prediction Error	0.75%	3.76%	0.17%	15.16%	4.25%	0.13%	3.08%	0.57%	0.22%	0.70%

Table 3. Prediction Results of GCR Characterisation Model

Model Parameters		w=1 $\gamma=1$	w=1 $\gamma=2$	w=1 $\gamma=3$	w=0.8 $\gamma=2$	w=0.6 $\gamma=1$	w=0.6 $\gamma=2$
RRMS	Max	0.0284	0.0386	0.0448	0.0406	0.0358	0.0450
	Mean	0.0057	0.0046	0.0066	0.0124	0.0223	0.0238
	Median	0.0025	0.0025	0.0027	0.0136	0.0311	0.0321
CIELAB (D50/2°)	Max	17.2222	3.9307	14.4710	26.3003	18.2924	18.9033
	Mean	1.6288	1.2318	1.5599	2.7461	6.7704	7.0959
	Median	0.6712	0.5982	0.6675	1.8779	6.0762	6.5567
CIEDE2000 (D50/2°)	Max	14.8280	3.3559	12.6096	17.2390	16.1372	16.3735
	Mean	1.2030	0.9620	1.2164	2.1967	6.2064	6.4506
	Median	0.5841	0.5934	0.6824	1.5111	4.9186	5.1463

$$D_{\mathrm{CMY}}(\lambda) = D_{\mathrm{CMY}}(\lambda)_i + \frac{[D_{\mathrm{CMY}}(\lambda)_{i+1} - D_{\mathrm{CMY}}(\lambda)_i][D(\lambda) - f_i(D_{\mathrm{K}}(\lambda)]}{f_{i+1}[D_{\mathrm{K}}(\lambda)] - f_i[D_{\mathrm{K}}(\lambda)]}$$
$$\text{when } f_i[D_{\mathrm{K}}(\lambda)] < D(\lambda) < f_{i+1}[D_{\mathrm{K}}(\lambda)], i = 1, 2, \cdots, 9, \quad (9)$$

$$D_{\mathrm{CMY}}(\lambda) = D_{\mathrm{CMY}}(\lambda)_1, \text{ when } D(\lambda) < f_1[D_{\mathrm{K}}(\lambda)]; \quad (10)$$

$$D_{\mathrm{CMY}}(\lambda) = D_{\mathrm{CMY}}(\lambda)_{10}, \text{ when } D(\lambda) > f_{10}[D_{\mathrm{K}}(\lambda)]; \quad (11)$$

$$D_{\mathrm{CMY}}(\lambda) = D_{\mathrm{CMY}}(\lambda)_i, \text{ when } D(\lambda) = f_i[D_{\mathrm{K}}(\lambda)], i = 1, 2, \cdots, 10. \quad (12)$$

The 3-ink density D_{CMY} (λ) is transferred back into the spectral reflectance $R_{\mathrm{CMY}}(\lambda)$ to predict the CMY normalised values based on the inverse cellular Yule-Nielsen spectral Neugebauer (CYNSN) model[8,9]. The inverse CYNSN model has been explored in detail in the previous study of the authors. The model was accomplished using the linear regression iteration[10,11] and cell searching algorithm[12]. Hereto, all the CMYK normalised values are obtained and the GCR characterisation model is established.

To investigate the model performance, 120 grid testing colour patches were printed and measured by Spectrolino spectrophotometer. The prediction results, with different w and γ values in Eq. (8), were evaluated in terms of reflectance root mean square error (RRMS)[12] as well as CIELAB and CIEDE2000 colour difference, as shown in Table 3.

In Table 3, the best model performance was achieved when w=1, γ=2. The prediction errors under this set of model parameters are presented in Fig. 5, where the horizontal axis represents the testing sample number. The increase in the error raised the K values of the actual testing samples used for printing. The prediction errors were very small for the samples with low and high K values while peak errors occurred for the samples with moderate K values. The use of the quadratic function with positive quadratic term coefficients of w=1 and γ=2 to calculate GCR percentage p in Eq. (8) accounts for this phenomenon.

In the case of model parameters with w=1 and γ=2, the average RRMS error was only 0.46%, and the RRMS of most samples was below 1%, which indicated precision of the proposed GCR characterisation method in the reproduction of spectral reflectances of target colours. Likewise, the CIELAB colour difference mean of 1.2318 and max value of 3.9307, together with the CIEDE2000 colour difference mean of 0.9620 and max value of 3.3559 showed high colorimetric prediction accuracy compared with those of other published studies. The GCR method of Kang[4], which aimed at spectral fit, achieved the prediction accuracy mean of 3.11 and maximum 5 CIELAB units. In the study of Zeng[3], a higher accuracy mean of 0.8 and maximum 2.4 CIELAB units were accomplished by focusing on direct colorimetric mapping. However, the issue of avoiding metamerism was not considered in this letter. Compared with these two methods, the proposed method in the current study showed fine spectral and colorimetric prediction accuracy simultaneously. Therefore, the feasibility of this proposed GCR characterisation model has been verified.

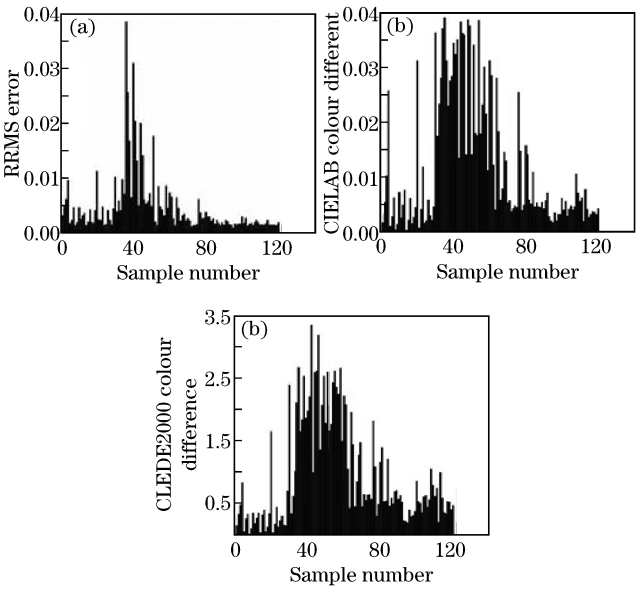

Fig. 5. Histograms of the GCR characterisation model prediction results with w=1 and γ=2 (D50/2°) (a) RRMS, (b) CIELAB, and (c) CIEDE2000.

In conclusion, a novel GCR characterisation model is proposed. The model only requires building the CMY 3D CYNSN model, black ink 1D LUT, and sub-additivity equations. Compared with the CMYK 4D CYNSN model, the number of training samples is significantly decreased due to the dimensionality reduction. Based on the deduced spectral density sub-additivity equations, the additivity failure is effectively corrected and the colour printer characterisation model with high spectral and colorimetric prediction accuracy is accomplished. This methodology could also be applied to multi-ink printing system besides the CMYK 4-ink printer to simplify the CYNSN model and reduce metamerism.

References

1. D. Littlewood and G. Subbarayan, J. Imaging Sci. Technol. **46,** 533 (2002).
2. R. Balasubramanian and R. Eschbach, J. Imaging Sci. Technol. **45,** 152 (2001).
3. H. Zeng, Proc. SPIE **3963,** 317 (2000).
4. H. Kang, Proc. SPIE **2171,** 287 (1994).
5. Y. Wang and H. Xu, Chin. Opt. Lett. **3,** 725 (2005).
6. R. W. G. Hunt, *the Reproduction of Colour* (John Wiley and Sons, Ltd., England, 2006), pp. 221–239.
7. S. Bandyopadhyay, T. Paul, and S. Bandyopadhya, in *Proceedings of 22nd International Conference on Digital Printing Technologies* 367 (2006).
8. D. Wyble and A. Kraushaar, Col. Res. Appl. **30,** 322 (2005).
9. D. R. Wyble and R. S. Berns, Col. Res. Appl. **25,** 4 (2000).
10. P. Urban and R. R. Grigat, Col. Res. Appl. **31,** 229 (2006).
11. C. Li and M. R. Luo, in *Proceedings of CIC16* 84 (2008).
12. J. Guo, H. Xu, and M. R. Luo, Chin. Opt. Lett. **8,** 1106 (2010).